Electronic Supplementary Material (ESI) for Physical Chemistry Chemical Physics

Electronic Supplementary Material

Reaction dynamics of CN radicals with tetrahydrofuran in liquid solutions

R.A. Rose,[1‡] S.J. Greaves,[1] F. Abou-Chahine,[1] D.R. Glowacki,[1,*] T.A.A. Oliver,[1#] M.N.R. Ashfold,[1] I.P. Clark,[2] G.M. Greetham,[2] M. Towrie[2] and A.J. Orr-Ewing[1,*]

(1) *School of Chemistry, University of Bristol, Cantock's Close, Bristol BS8 1TS, UK*

(2) *Central Laser Facility, Research Complex at Harwell, Science and Technology Facilities Council, Rutherford Appleton Laboratory, Harwell Science and Innovation Campus, Didcot, Oxfordshire, OX11 0QX, UK*

‡ Current address: *RAL Space, Science and Technology Facilities Council, Rutherford Appleton Laboratory, Harwell Science and Innovation Campus, Didcot, Oxfordshire, OX11 0QX, UK*

Current address: *Department of Chemistry, University of California, Berkeley, CA 84720, USA.*

* Authors for correspondence

Tel: +44 117 9287672

Fax: +44 117 9250612

e-mail: a.orr-ewing@bris.ac.uk

david.r.glowacki@bris.ac.uk

Analytical form of the reaction potential energy surface

The potential energy surface (PES) for the CN-radical abstraction of an H-atom from tetrahydrofuran (THF) was represented as a coordinate-dependent Hamiltonian, $\boldsymbol{H}(\mathbf{q})$, using a symmetric $n \times n$ matrix, where the diagonal elements, $V_i(\mathbf{q})$, are the molecular mechanics energies for a particular connectivity arrangement, and ε_i are corresponding energy offsets associated with reaction endo- or exothermicity.[1] The overall potential energy of the system for a given set of nuclear coordinates is then taken as the lowest eigenvalue, $\lambda_0(\mathbf{q})$, of $\boldsymbol{H}(\mathbf{q})$. To model CN + c-$C_4H_8O$ → HCN + 3-C_4H_7O, we used a 2-state Hamiltonian of the form

$$H(\mathbf{q}) = \begin{pmatrix} V_1(\mathbf{q}) + \varepsilon_1 & H_{12}(\mathbf{q}) \\ H_{21}(\mathbf{q}) & V_2(\mathbf{q}) + \varepsilon_2 \end{pmatrix} \qquad \text{(S1)}$$

in which the off-diagonal coupling elements are identical ($H_{12}(\mathbf{q}) = H_{21}(\mathbf{q})$). State 1 corresponds to the reactant connectivity, and state 2 corresponds to the product connectivity. The energy difference between the offsets, $\varepsilon_2 - \varepsilon_1$, was fixed to –26.1 kcal mol^{-1} based on the data in Table 1 of the main text.

Gradients of the energy eigenvalues with respect to Cartesian coordinates were calculated using the Hellman-Feynmann approach

$$\frac{d\boldsymbol{D}}{d\mathbf{q}} = \boldsymbol{U}^{\mathrm{T}} \frac{\mathrm{d}\boldsymbol{H}}{\mathrm{d}\mathbf{q}} \boldsymbol{U} \qquad \text{(S2)}$$

where $\boldsymbol{U}$ is the eigenvector matrix, and $\boldsymbol{D}$ is the diagonal eigenvalue matrix. The elements of $\boldsymbol{D}$, $\boldsymbol{U}$, and $\boldsymbol{H}$ all implicitly depend on $\mathbf{q}$. Equation (S2) is accurate so long as the elements of $\boldsymbol{H}(\mathbf{q})$ are continuously differentiable in the neighbourhood of $\mathbf{q}$.[2]

The system under investigation here involves non-equilibrium relaxation dynamics, so that an accurate representation of the shape of the energy profile along the reaction path is important to obtain reliable results. This requirement places considerable significance on the evaluation of the off-diagonal coupling elements in equation (S1), since they determine the shape of the energy profile. Our method for calculating the off-diagonal terms is similar in philosophy to the recently described distributed Gaussian approach,[3] with the $H_{12}(\mathbf{q})$ fitted to gas-phase electronic structure theory results for some dynamically significant subset of **q**. We represented the off-diagonal coupling elements as a linear combination of two Gaussian functions of the H11–CN bond distance, *r* – *i.e.*,

$$H_{12}(r) = \sum_{i=1}^{2} A_{12}^{i} exp\left(-\frac{1}{2}\left(\frac{\left(r - B_{12}^{i}\right)}{C_{12}^{i}}\right)^{2}\right) \qquad \text{(S3)}$$

where A_{12}^{i}, B_{12}^{i} and C_{12}^{i} are the respective amplitude, centre, and width parameters for the *i*th Gaussian function describing the off-diagonal term that couples state 1 and 2. Equation (S3) generates a total of six parameters which we fitted using a Levenberg-Marquardt non-linear least squares optimization algorithm to the H11-CN relaxed scans shown in Figure 2 of the main text. The goodness of fit was determined from a simple merit function

$$\chi^{2}(A_i, B_i, C_i; i \in k) = \sum_{r \in path} \left[\frac{\lambda_0(\mathbf{q}=r) - \left(\Delta E_{CCSD\ (T)}(r)\right)}{\Delta E_{CCSD\ (T)}(r)}\right]^{2} \qquad \text{(S4)}$$

where $\Delta E_{CCSD(T)}(r) = E_{CCSD(T)}(r) - E_{CCSD(T)}(\infty)$ is the CCSD(T) energy at some reaction separation r with the reference energy being that at $r \to \infty$. Equation (S4) was found to weight satisfactorily both the low and high energies along the reaction path in Figure 2. For each trial set of parameters defining the $H_{12}(\mathbf{q} = r)$ coupling elements, values of $\lambda_0(\mathbf{q} = r)$

were obtained through geometry optimization with the H–CN coordinate, *r*, constrained to be identical to the corresponding value of *r* along the CCSD(T) reaction path. Hence, the structures are not necessarily identical to those used in the CCSD(T) scans. However, inspection of both sets of structures along the reaction path shows that they are very similar. The parameters for the optimized Gaussian functions are given in Table S1, with the resultant energies along the H11-CN reaction coordinate shown in Figure 2. The analytical PE function resulting from these calculations was used in computation of trajectories for reaction (1) in solution in THF, as is described in section 4.5 of the main paper.

All force field evaluations discussed in this paper were obtained using a locally modified version of the CHARMM software suite,[4] to which we have recently added code for carrying out reactive molecular dynamics with a generic *n*-state Hamiltonian matrix. In this work, diagonal elements of the 2-state Hamiltonian matrix in equation (S1) were calculated using the Merck Molecular Mechanics force field (MMFF),[5] which we modified to treat sp^2 radicals. Fitting was carried out using a script to interface CHARMM with the Levenberg-Marquardt implementation available within the Scientific Python (SciPy) library.

i	A_{12}^i / kcal mol^{-1}	B_{12}^i (centre) / Å	C_{12}^i (width) / Å
1	8.496	1.783	0.188
2	105.852	2.602	2.172

Table S1: Optimized parameters for the Gaussian functions making up H_{12} in Eqs (S1) and (S3).

Relaxation timescales for vibrationally excited HCN in solution in THF

Spectral overlap with solvent bands prevents time-resolved IR absorption measurements for HCN reaction products in neat THF in the C–H stretching region, suggesting that the ν_3 band shifts significantly in solution from its gas phase value. In the standard MMFF setup, ν_3 has a gas phase value of 3470 cm^{-1} (which can be compared to a spectroscopically determined value of 3444 cm^{-1} and a 3_0^1 band transition frequency of 3311 cm^{-1} from ref. 6). Here, we consider the consequences of the choice of the C–H stretch frequency in the MD simulations for the rate of vibrational relaxation of nascent HCN(001) from reaction of CN radicals with THF, as discussed in section 4.5.2 of the main paper.

Letting $\boldsymbol{v}$ represent the vector of atomic velocities in a particular dynamics simulation, the vibrational spectrum, $F(\omega)$, of an arbitrary subset of atoms may be obtained as the fast Fourier transform (FFT) of a correlation function obtained from averaging over time series of the vector dot products, $\langle \boldsymbol{v}(0) \cdot \boldsymbol{v}(t) \rangle$:[7]

$$F(\omega) = \frac{1}{2\pi} \int_{-\infty}^{\infty} dt\, e^{i\omega t}\, \langle \boldsymbol{v}(0) \cdot \boldsymbol{v}(t) \rangle \qquad \text{(S5)}$$

where angled brackets indicate an average. Figure S1 shows that the THF spectrum obtained from our NVE dynamics simulations compares reasonably well with that obtained from an experimental measurement at room temperature (using a 12 μm thick sample of THF).

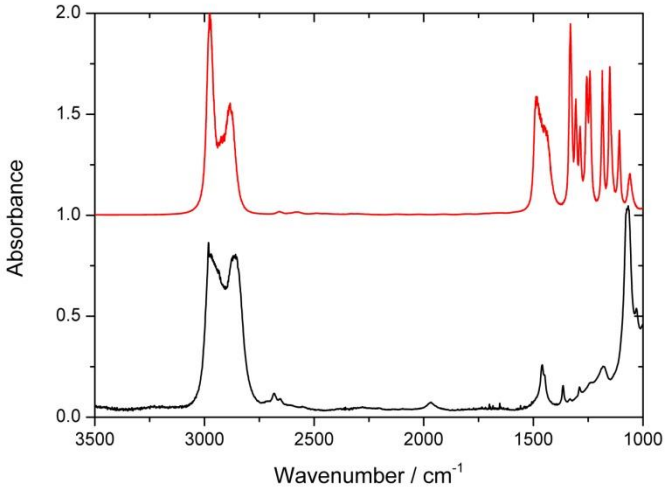

Figure S1: comparison of an experimental IR spectrum of liquid THF at room temperature (black) with that obtained from molecular dynamics simulations at 298 K (red). The calculated spectrum has been scaled to a maximum absorbance of unity and offset vertically for clarity.

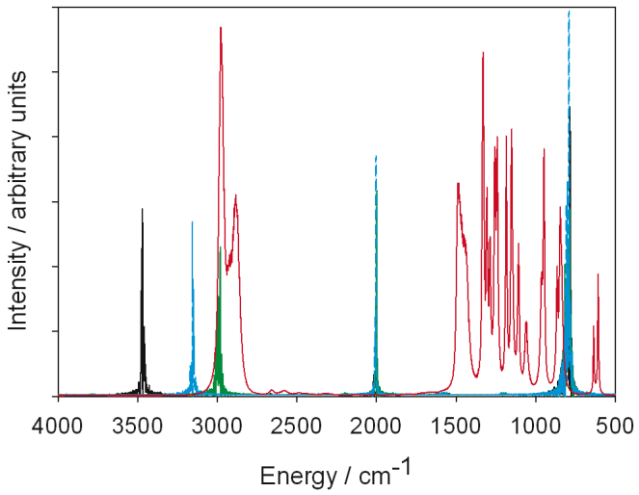

Figure S2: Comparison of the THF solvent spectrum from our MMFF MD simulations (red) and the HCN spectrum obtained from the standard MMFF setup (black). The blue and green plots show HCN spectra obtained following modification of the H–CN force constant as described in the text. Peaks in the range 3000 – 3500 cm^{-1} are the ν_3 mode whereas those at lower wavenumber correspond to ν_1 and ν_2 and are little affected by changes to the H–CN force constant.

However, the spectral shift of HCN (ν_3) in THF is not well described by the standard MMFF force field setup. Figure S2 shows the computed HCN spectrum in a THF solvent as a black curve, and the vibrational band peaks at 3468 cm^{-1}. This observation is important because the MD-calculated HCN(001) relaxation timescale in THF depends sensitively on the extent to which the HCN 3_0^1 band overlaps the THF spectral band seen between 2900 and 3000 cm^{-1}. To demonstrate this dependence, we ran three sets of simulations of HCN in THF in which we decreased the value of the H–CN stretching force constant. Figure S2 shows an overlay of the experimental THF solvent spectrum (red) with the HCN spectra obtained in each of the three sets of simulations. Our force constant modifications resulted in the C-H stretching mode of HCN taking frequency values of ν_3~3468 cm^{-1}, ~3155 cm^{-1}, and ~3000 cm^{-1}. The respective HCN peaks corresponding to ν_1 and ν_2 at ~784 and ~2004 cm^{-1} do not change significantly with changes to the H–CN force constant. The consequences of these changes in overlap of the HCN 3_0^1 band frequency for computed vibrational relaxation rates of HCN(001) in THF are discussed in section 4.5.2 of the main paper.

References

1 D. R. Glowacki, A. J. Orr-Ewing and J. N. Harvey, *J. Chem. Phys.*, 2011, **134**, 204311.
2 P. Lancaster, *Numerische Mathematik*, 1964, **6**, 377-387.
3 K. F. Wong, J. L. Sonnenberg, F. Paesani, T. Yamamoto, J. Vanicek, W. Zhang, H. B. Schlegel, D. A. Case, T. E. Cheatham, W. H. Miller and G. A. Voth, *J. Chem. Theory Comput.*, 2010, **6**, 2566-2580.
4 B. R. Brooks, C. L. Brooks, III, A. D. Mackerell, Jr., L. Nilsson, R. J. Petrella, B. Roux, Y. Won, G. Archontis, C. Bartels, S. Boresch, A. Caflisch, L. Caves, Q. Cui, A. R. Dinner, M. Feig, S. Fischer, J. Gao, M. Hodoscek, W. Im, K. Kuczera, T. Lazaridis, J. Ma, V. Ovchinnikov, E. Paci, R. W. Pastor, C. B. Post, J. Z. Pu, M. Schaefer, B. Tidor, R. M. Venable, H. L. Woodcock, X. Wu, W. Yang, D. M. York and M. Karplus, *J. Comput. Chem.* , 2009, **30**, 1545-1614.
5 T. A. Halgren, *J. Comput. Chem.*, 1996, **17**, 490-519.
6 A. M. Smith, S. L. Coy, W. Klemperer and K. K. Lehmann, *J. Mol. Spectrosc.*, 1989, **134**, 134-153.
7 Y. Yamauchi, H. Nakai and Y. Okada, *J. Chem. Phys.*, 2004, **121**, 11098-11103.